

## MERLIN and VLA observations of compact steep-spectrum radio sources

R. E. Spencer, J. C. McDowell and M. Charlesworth

*Nuffield Radio Astronomy Laboratories, University of Manchester, Jodrell Bank, Macclesfield, Cheshire, SK11 9DL*

C. Fanti *Departimento di Astronomia, Universita di Bologna, Bologna, Italy and Istituto di Radioastronomia, Universita di Bologna, Via Irnerio 46, I401266 Bologna, Italy*

P. Parma *Istituto di Radioastronomia, Universita di Bologna, Via Irnerio 46, I401266 Bologna, Italy*

J. A. Peacock *Royal Observatory, Blackford Hill, Edinburgh, EH9 3HJ*

Accepted 1989 March 21. Received 1989 March 21; in original form 1988 November 23

**Summary.** We present maps made with MERLIN and the VLA of compact steep-spectrum radio sources at wavelengths of 18, 6 and 2 cm with sub-arcsecond resolution. The sources were selected from the 3C and Peacock & Wall surveys. Study of the angular structures found shows that the high-frequency survey of Peacock & Wall preferentially selects sources with angular sizes of  $< 0.1$  arcsec, even though their high-frequency spectra are still steep. The resolved quasars in this study have predominantly complex or distorted structures, whereas the galaxies tend to have simpler ‘double’ type structures.

### 1 Introduction

Studies of extragalactic radio sources have shown that the two main classes, those with flat or steep radio spectra, generally have distinctive structures. The flat-spectrum ( $\alpha < 0.5$ ,  $S \propto \nu^{-\alpha}$ ) sources have structures dominated by compact cores, resolvable only by VLBI techniques, and sometimes lower-brightness jets also (Davis, Stannard & Conway 1977); they are typified by the quasar 3C 273 (Davis, Muxlow & Conway 1985). The steep-spectrum sources ( $\alpha \geq 0.5$ ) tend to have the classical ‘double’ structure with extended outer lobes and a relatively weak core, e.g. Cygnus A (Hargrave & Ryle 1974; Perley, Dreher & Cowan 1984). The latter sources are selected predominantly by source surveys at low frequencies such as the 178-MHz 3C survey and have been studied extensively by aperture synthesis instruments. We note, nevertheless, that the median angular size of the steep-spectrum sources in the 3CR 166 source sample by Jenkins, Pooley & Riley (1977) is 28 arcsec and that 20 per cent have angular

sizes of less than 5 arcsec. These small-diameter sources have had less study, because of the resolution limitations of synthesis arrays such as the Cambridge 5-km telescope. We note further that recent studies at 2.7 GHz by Peacock & Wall (1981), hereafter PW1, have shown that, not only are the sources with flat high-frequency spectra compact, but a large proportion (31 per cent) of the steep high-frequency spectrum sources are also unresolved ( $< 2$  arcsec) with the Cambridge 5-km telescope (Peacock & Wall 1982, hereafter PW2; Kapahi 1981). This value compares with 14 per cent for the 3CR sources which were selected at 178 MHz.

These relatively small objects with steep spectra have become known as either 'Compact Steep Spectrum' sources (CSS) or 'Steep Spectrum Cores' (SSC) and some have been recently studied with the VLA (van Breugel, Miley & Heckman, 1984; Pearson, Perley & Readhead 1985), MERLIN and VLBI (Wilkinson *et al.* 1984b; Fanti *et al.* 1985). Van Breugel *et al.* (1984) found that the majority of the CSS sources in their sample have structure on a scale of more than 0.05 arcsec. The more extended objects sometimes show complex structures which van Breugel *et al.* ascribe to interaction of jets with dense galactic environments.

This paper reports MERLIN observations at a wavelength of 18 cm on a larger sample of 42 such sources from 3C and PW2 lists, together with VLA observations at 6 and 2 cm on the PW2 sample. The sources do not form a complete sample limited by size or flux density; the selection arose from an amalgamation of separate proposals for MERLIN observations containing many sources in common.

There were three broad criteria used in source selection: first, the steep-spectrum sources from the 3CR catalogue which were known at the time of the observations to have angular sizes of  $< 5$  arcsec; secondly, those steep-spectrum 3CR sources which had  $> 80$  per cent of their emission from a region of  $< 10$  kpc in projected linear size (Fanti *et al.* 1985); and thirdly the steep-spectrum sources from PW1 which were unresolved by the Cambridge 5-km telescope (resolution  $\sim 2$  arcsec). Some of the members of the latter sample have been observed by MERLIN at 18 cm by other observers; we do not present 18-cm data for these sources, but give the relevant references in Table 1. The Peacock & Wall sample forms a group which has been selected by angular size, flux density at 2.7 GHz and spectral index ( $\alpha_{\text{HF}} \geq 0.5$ , measured between 2.7 and 5 GHz) only. Combination of our results with those published by other authors for the 3CR sample enables us to form a sample similarly complete, but selected at the lower observing frequency of 178 MHz, so that comparisons can be made. These two samples are discussed in Section 4.

CSS sources have projected linear sizes of  $< 20$  kpc, and the number of such sources cannot be explained simply by projection effects alone. The expected number of projected sources from the more extended ( $> 5$  arcsec) population is much smaller than the observed number of CSS (Fanti *et al.* 1988). They must be physically small, and within the envelope of any parent galaxy. Gas densities are likely to be high in such regions and we may expect to see the results of interactions of any jets in the sources with this gas. The correlations between radio structure and optical line emission from the narrow-line region found in active galaxies (Heckman, Miley & Green 1984; Pedlar *et al.* 1987) also indicate such interactions. The consequences of a gas-rich environment are also discussed in Section 4.

## 2 Observations

The sources in the combined lists (3C and PW) were observed with the six-telescope MERLIN system at 18 cm during 1982 October and November. The PW sample was also observed with the VLA at 6 and 2 cm during 1982 June.

The MERLIN observations used the Mk II, Tabley, Darnhall, Wardle, Knockin and Defford telescopes, giving a maximum baseline of 132 km. The sources are strong enough not to

require full synthesis observations to achieve good signal-to-noise ratios. They were therefore arranged into groups of 2 or 3 with close positions on the sky and observed for 30 or 20 min each, cycling through the group once per hour. The group was followed for  $\sim 12$  hr, giving the full range of UV coverage. This technique enabled a large number of sources to be observed in the limited observing time available. The small angular size of the sources meant that short breaks in the hour angle coverage gave no significant loss of structural information. The baselines were calibrated by daily short observations of the unresolved source BL Lac. Offsets in the closure phase and closure amplitude due to correlator errors were corrected in this procedure. The flux density scale was established by observations of 3C 48 (flux density 13.85 Jy, Baars *et al.* 1977) every 2 or 3 d, using data from the three short-baselines (Mk II, Tabley and Darnhall) only, since 3C 48 is resolved on the longest MERLIN baseline.

The MERLIN data were analysed by using the hybrid mapping technique (Readhead & Wilkinson 1978; Cornwell & Wilkinson 1981), starting from a point-source model and using several cycles of telescope phase correction (CORTEL), Fourier inversion and CLEAN (Högbom 1974) in the OLAF analysis system on the Jodrell Bank Starlink VAX. Only the first few positive flux values from CLEAN were used in the initial cycles (the Clark algorithm, see Cornwell & Wilkinson 1983). Later cycles allowed the telescope gains as well as phases to be corrected. The processed UV data were then mapped using standard AIPS routines. This method produced satisfactory maps in most cases, with dynamic ranges (peak brightness to lowest believable contour) of typically 300:1. Some sources (3C 213.1, 318, 343, 343.1) were reprocessed using the difference mapping technique (Cornwell & Wilkinson 1983).

The VLA observations were made in A configuration yielding a maximum baseline of 36.4 km. The data were calibrated using the Baars *et al.* (1977) flux density value of 3C 286. The maps were made using the standard AIPS routines. Two iterations of the ASCAL self-calibration routine were used to correct telescope-dependent phase and amplitude errors.

### 3 Results

The sources observed with MERLIN and the VLA are listed in Table 1. The table also contains sources which were not observed by us. These sources complete a sample of compact ( $< 2$  arcsec) steep-spectrum sources selected from the 3CR low-frequency (178 MHz) survey for comparison with the higher-frequency (2.7 GHz) sample of PW2 (see Section 4). An indication of the parent sample is given in the table (PW if PW2, C if 3CR) together with optical identification, largest angular size (from our data where available or else from the reference given) and structure as described below. Composites of the maps are given in Fig. 1. Only sources significantly resolved at one or more frequencies are shown in the figures, and in some cases the MERLIN or VLA data are not available to us. Noise levels were typically 1–2 mJy in the MERLIN data and 0.5–1 mJy in the VLA data. Circular restoring beams of FWHM of 0.3, 0.5 and 0.15 arcsec were used at 18, 6 and 2 cm, respectively. The maps are contoured logarithmically with the bottom contour at 5 times the rms level away from the source. The contours are plotted at levels of 1, 2, 4, 8, 16, 32, etc. times the minimum contour level.

Table 2 lists the peak brightness (in Jy beam<sup>-1</sup>) and minimum contour level (in mJy beam<sup>-1</sup>) for the maps of the resolved sources shown in Fig. 1. Table 3 lists the sources which are unresolved and are not plotted in Fig. 1, together with their total flux densities measured in our observations. Typical errors amount to 3–5 per cent. Parameters derived from the maps are given in Table 4. In appropriate cases the component sizes at half power,  $\omega_1$  and  $\omega_2$ , were derived by fitting elliptical Gaussian brightness distributions, either to the maps for the well-resolved sources or to the visibility data for the more compact sources. The angular sizes of the very extended sources where model fitting was inappropriate were measured from the maps

Table 1. Compact steep-spectrum sources from the 3C and PW surveys.

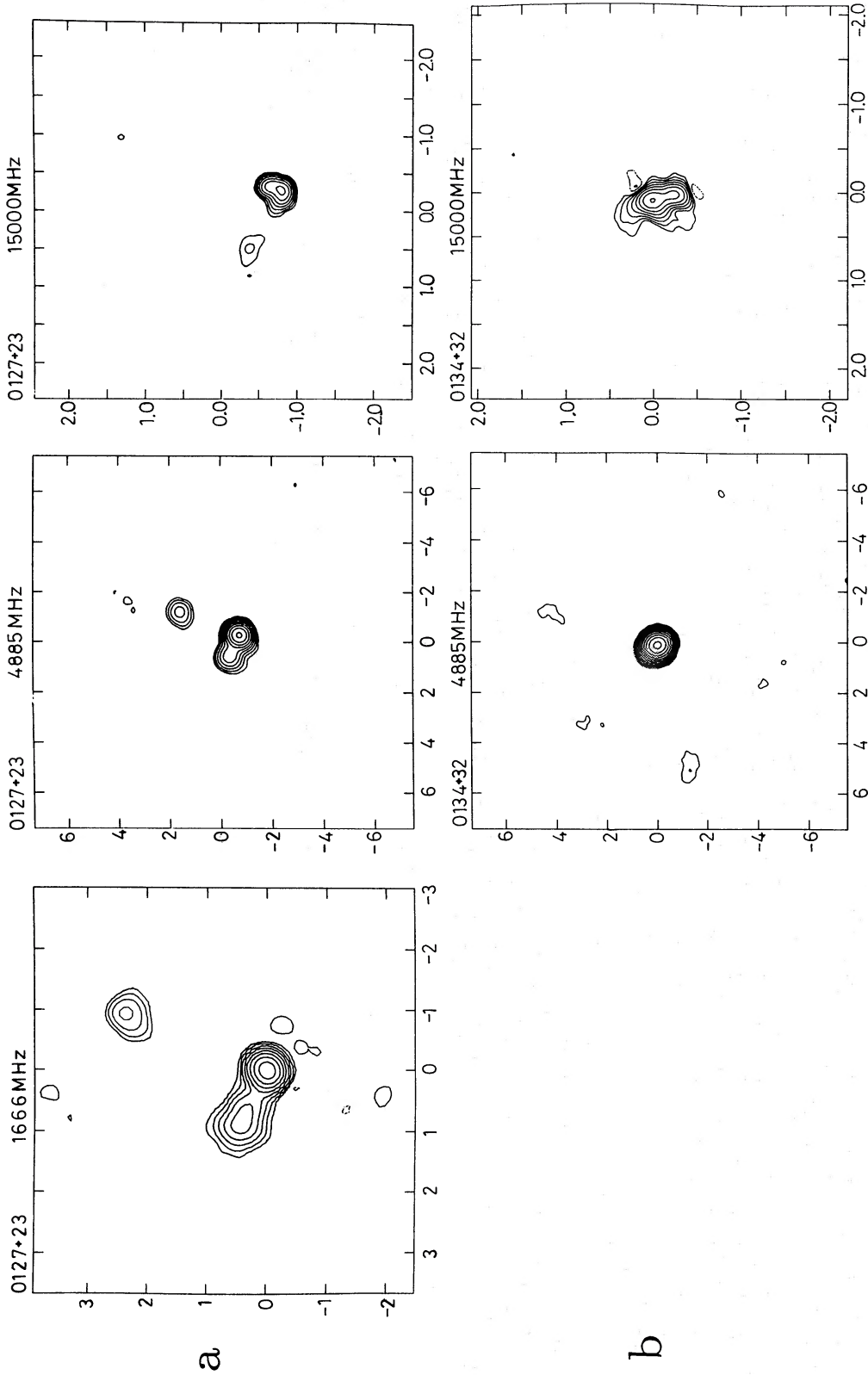
Name	Sample	id	z	morph	ref	lum log(p)	turn MHz	LAS	
0116+31	4C31.04	PW	G	0.059	P	23.80	550	<0.1	
0127+23	3C43	PWC	Q	1.47	C	26.54	<22	2.6	
0134+32	3C48	PWC	Q	0.367	C	26.06	70	1.3	
0138+13	3C49	PWC	G	0.621	D	25.75	100	1.0	
0221+27	3C67	PWC	G	0.310	D	25.20	<50	2.5	
0223+34	4C34.07	PW	Q?	1?	T	26.18	250	1.1	
0316+16	CTA21	PW	G?	1?	P	26.73	900	0.1	
0319+12	OE131	PW	Q	2.67	P	26.99	400	<0.1	
0345+33	3C93.1		G	0.244	S	24.85	60	0.2	
0404+76	4C76.03	PW	G	1.38	P	26.82	400	<0.1	
0428+20	OF247	PW	G?	0.219	S	25.12	1000	0.1	
0429+41	3C119		Q?	0.408	P	25.92	150	<0.1	
0518+16	3C138	PWC	Q	0.759	C	26.49	80	0.65	
0538+49	3C147	PWC	Q	0.545	C	26.56	140	1.4	
0658+38	3C173		G	0.292	D	24.87	30	2.6	
0740+38	3C186	C	Q	1.063	C	2	25.94	40	1.2
0758+14	3C190	C	Q	1.197	C	1	26.36	<20	2.6
0802+10	3C191	C	Q	1.956	C	2	26.72	<20	3.7
0858+29	3C213.1		G	0.194	D	24.52	60	9.0	
0908+43	3C216	C	Q	0.67	C	1	25.95	<20	3.0
1005+07	3C237		G	0.877	D	26.46	45	1.2	
1019+22	3C241	C	G	1.617	D	26.48	40	0.8	
1122+19	3C258		G	0.165	S	24.16	<178	0.1	
1143+50	3C266		G	1.275	D	26.14	100	4.5	
1153+31	4C31.38	PW	Q	1.577	D	26.69	100	0.9	
1203+64	3C268.3	PWC	G	0.371	D	25.43	<80	1.3	
1225+36	ON343	PW	Q?	1?	P	26.32	1000	<0.1	
1250+56	3C277.1	PW	Q	0.320	T	25.14	40	1.6	
1323+32	4C32.44	PW	G?	0.369	P	25.46	400	<0.1	
1328+30	3C286	PWC	Q	0.849	C	26.79	<50	3.8	

Table 1 – continued

Name	Sample	id	z	morph	ref	lum log(p)	turn MHz	LAS	
1328+25	3C287	PWC	Q	1.055	P	26.65	<38	<0.1	
1345+12	4C12.50	PW	G	0.122	P	24.67	500	<0.1	
1358+62	4C62.22	PW	G	0.429	P	25.64	600	<0.1	
1413+34	OQ323	PW	EF	1?	P	26.18	700	<0.1	
1416+06	3C298		Q	1.439	C	26.86	65	2.5	
1419+41	3C299	PWC	G	0.367	D	25.32	50	11.5	
1442+10	OQ172	PW	Q	3.53	P	27.33	1000	<0.1	
1443+77	3C303.1	C	G	0.267	D	24.77	70	2.0	
1447+77	3C305.1	C	G	1.132	D	26.14	90	2.8	
1458+71	3C309.1	PWC	Q	0.904	C	26.58	<20	2.2	
1517+20	3C318	C	G	0.752	T	25.91	<20	0.8	
1600+33	OS300	PW	EF	1?	P	26.31	1000	<0.1	
1607+26	CTD93	PW	G	0.47	P	25.79	1000	<0.1	
1634+62	3C343	PWC	Q	0.988	P	26.47	200	<0.1	
1637+62	3C343.1	PWC	G	0.750	D	26.15	200	0.3	
1641+17	3C346	C	G	0.161	C	3	24.72	<38	2.3
1819+39	4C39.56	PW	G?	0.4?	D	25.45	<178	1.0	
1828+48	3C380	C	Q	0.691	C	1	26.59	<20	1.5
1829+29	4C29.56	PW	Q?	2.51	T	27.13	<100	3.4	
2230+11	CTA102	PW	Q	1.037	T	26.64	900	2.6	
2247+14	4C14.82	PW	Q	0.237	S	24.87	<178	0.2	
2248+71	3C454.1		G	1.841	D	26.53	<20	1.6	
2249+18	3C454	C	Q	1.757	D	2	26.61	<38	0.6
2252+12	3C455		G	0.543	D	25.62	<38	4.0	
2342+82	PW	G	0.735	P		26.12	400	<0.1	

## Notes

PW: Peacock & Wall (1982). C: 3C, < 2 arcsec; “”: 3C other, for example  $|b| < 10^\circ$ . G: galaxy. Q: quasar. EF: empty field. P: point,  $< 0.1$  arcsec. S: single elongated component,  $> 0.1$  arcsec. D: double. T: three components in a line. C: complex, i.e.  $> 3$  components or bent  $> 20^\circ$ . lum:  $\log_{10}$  of the monochromatic luminosity in  $\text{W Hz}^{-1} \text{sr}^{-1}$  at 2.7 GHz, using the published redshift where available or the redshift estimated from the  $\nu$  magnitude if a galaxy; empty fields and quasars without a known redshift were assigned  $z=1$  ( $H_0 = 100 \text{ km s}^{-1} \text{ Mpc}^{-1}$ ,  $q_0 = 0.5$ ). turn: observed turnover frequency. References: 1. Pearson *et al.* (1985); 2. Cawthorne *et al.* (1986); 3. D. Stannard, private communication.



**Figure 1.** (a)-(aa) MERLIN and VLA maps of compact steep-spectrum sources. Contours are plotted at 1, 2, 4, 8, etc. times the bottom contour level which is at 5 times the rms noise level in the maps. Right ascension and declination scales are marked in arcsec. The sources are shown in right ascension order, with the MERLIN 1666-MHz first followed by the VLA maps at 4885.1 MHz and 14 964.5 MHz. A blank space generally occurs where data were not available to us. Exemptions to this occur in Fig. 1(k), (l), (s) and (aa), where only the MERLIN maps were available and the source maps are plotted consecutively to save space.

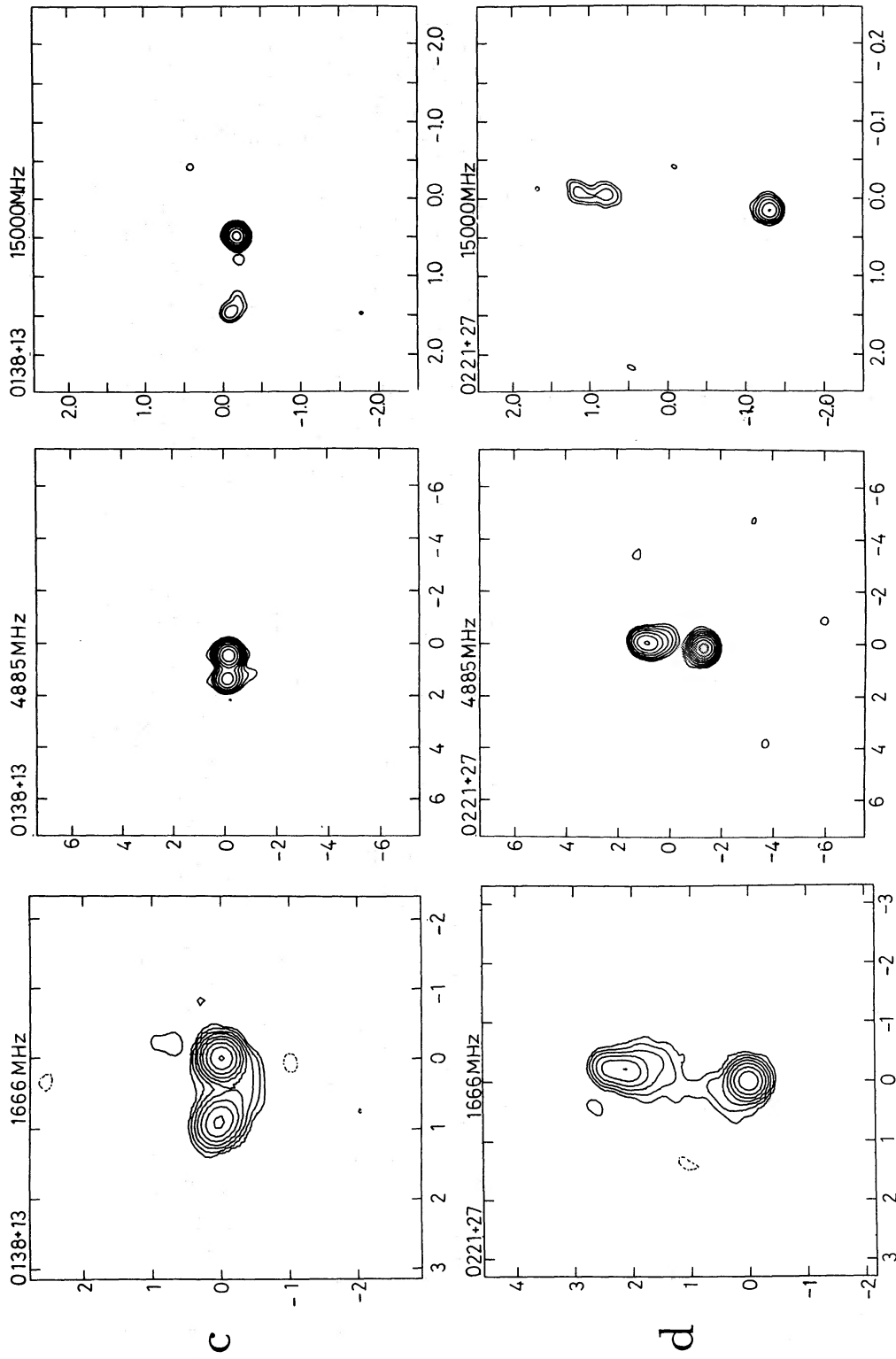


Figure 1 - continued

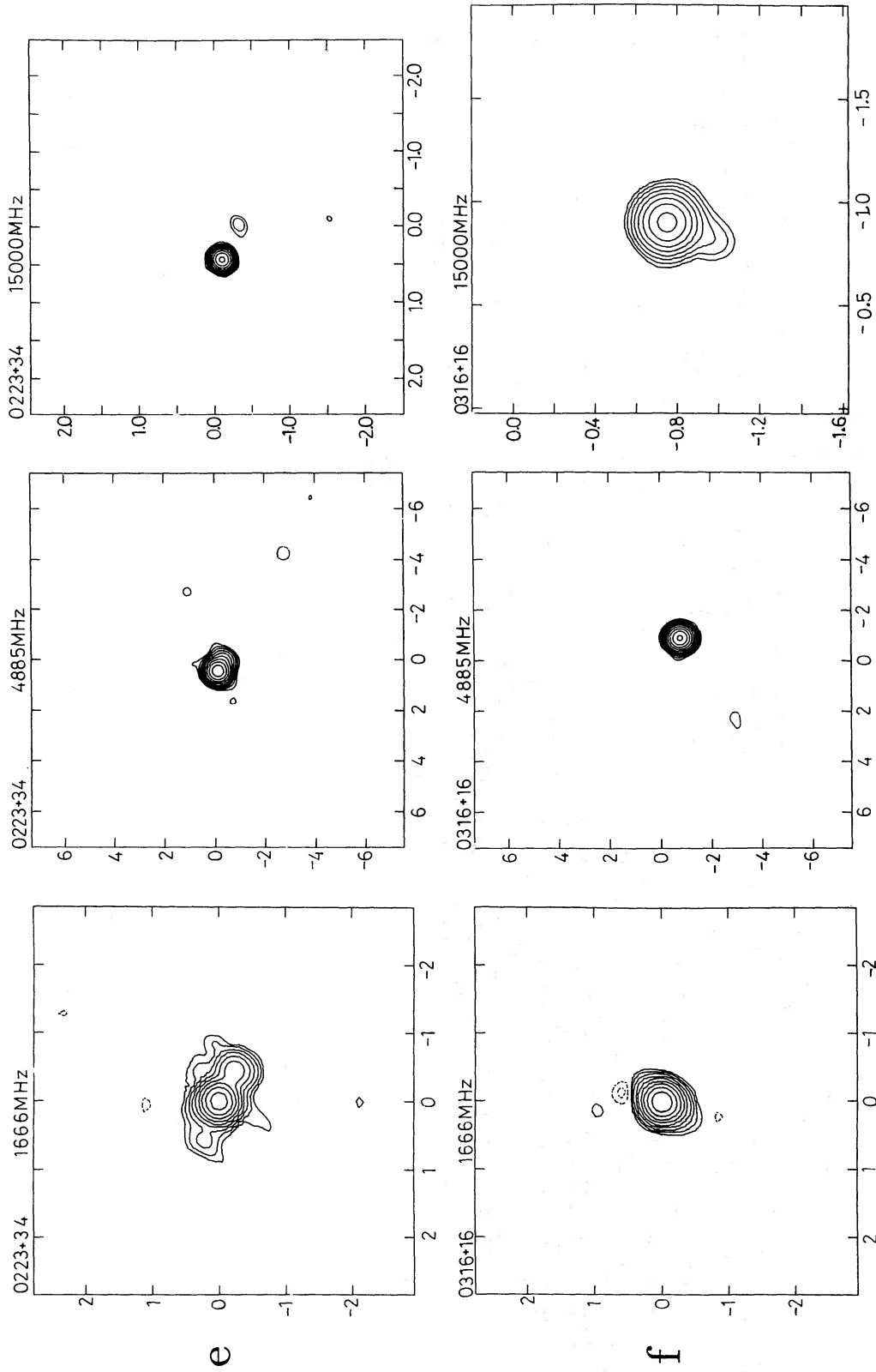


Figure 1 - continued

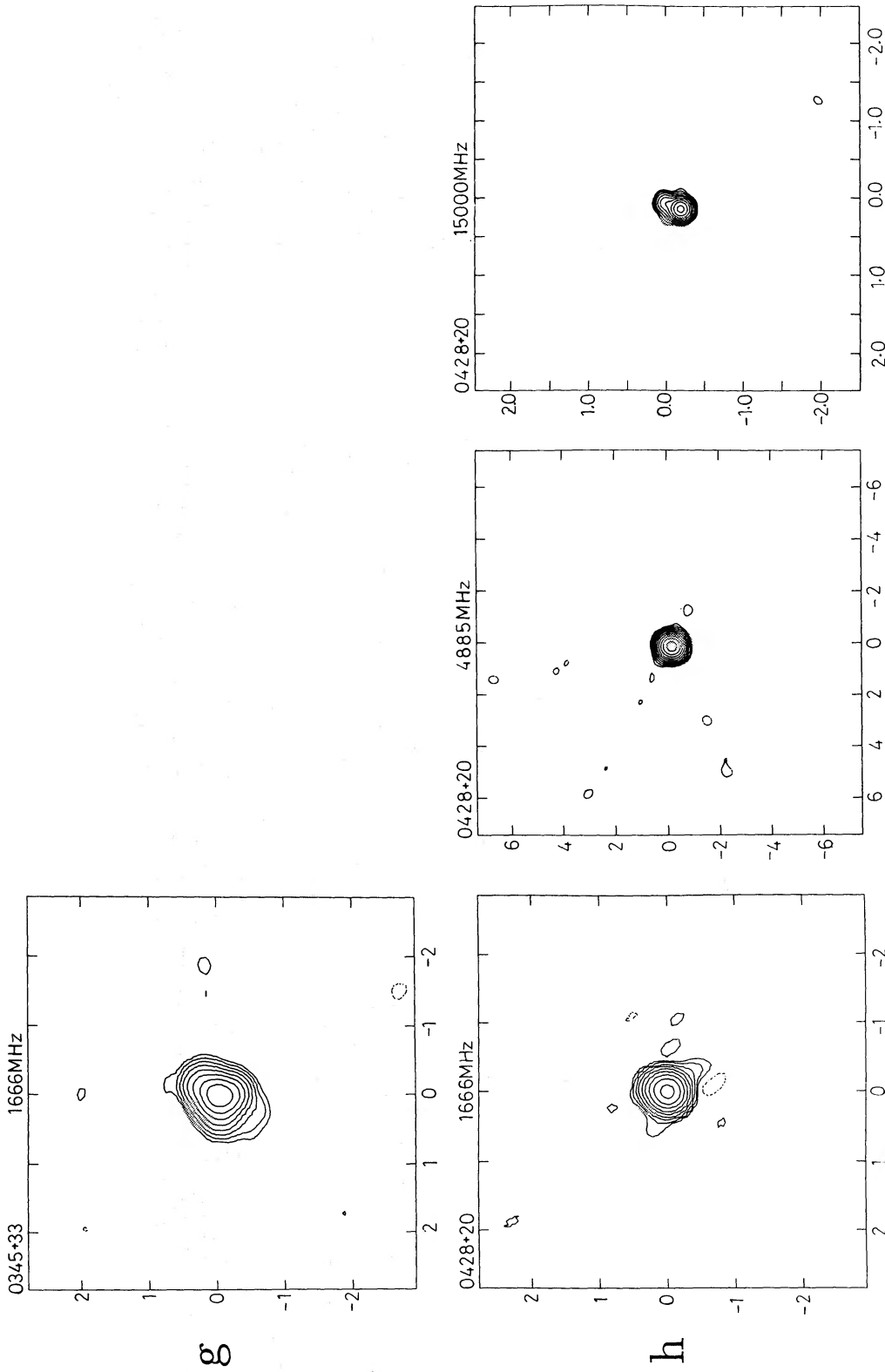


Figure 1 - continued

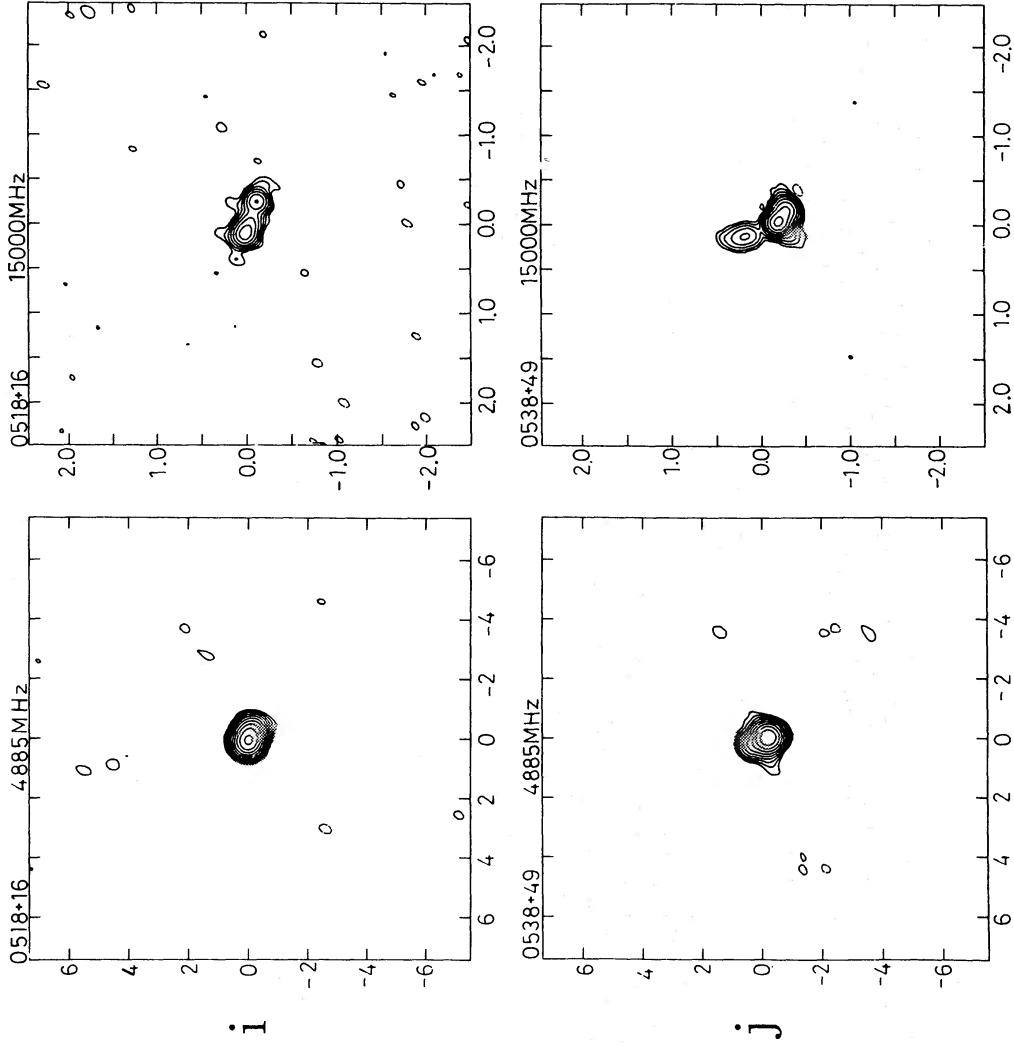


Figure 1 - continued

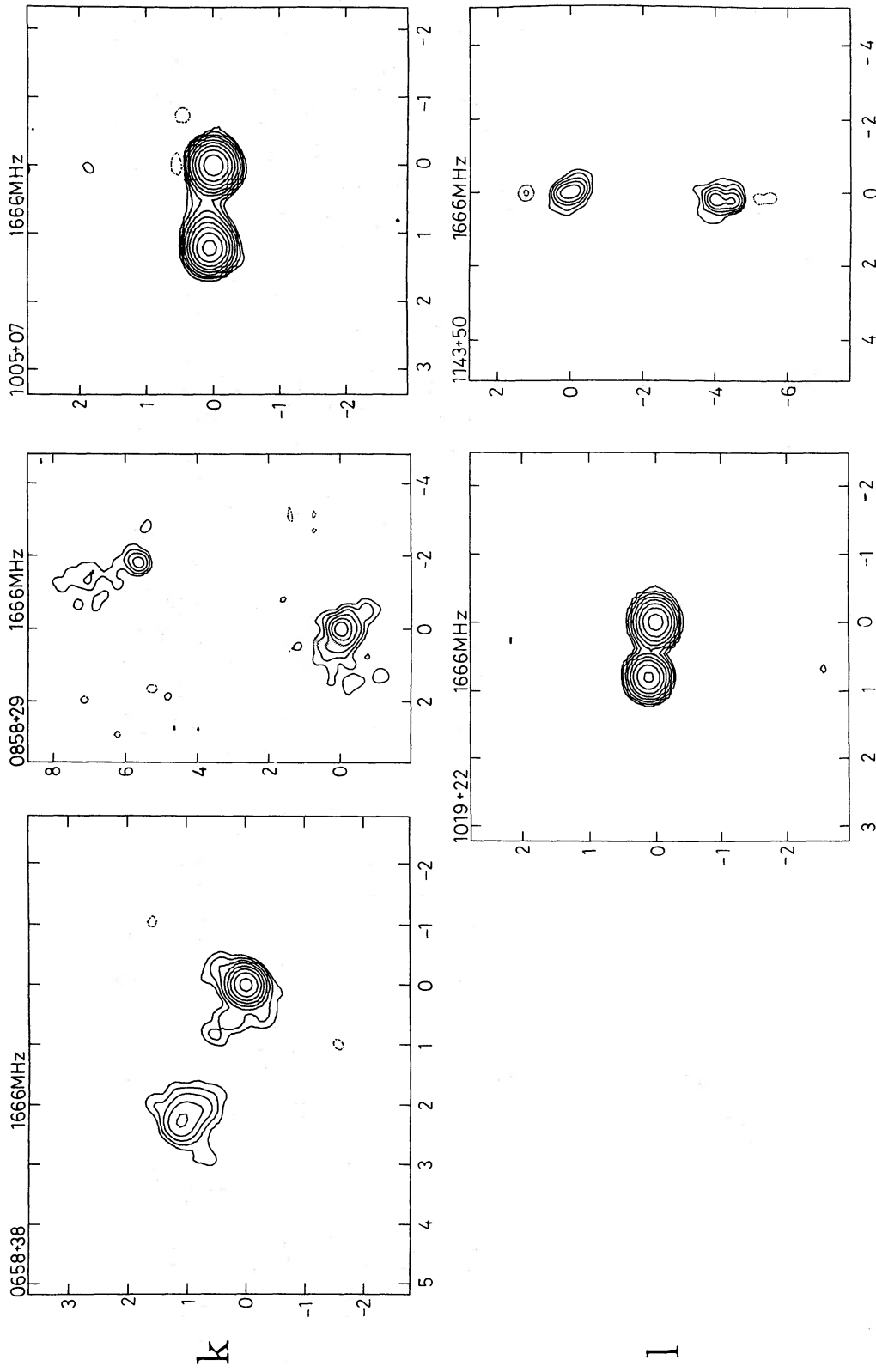


Figure 1 - continued

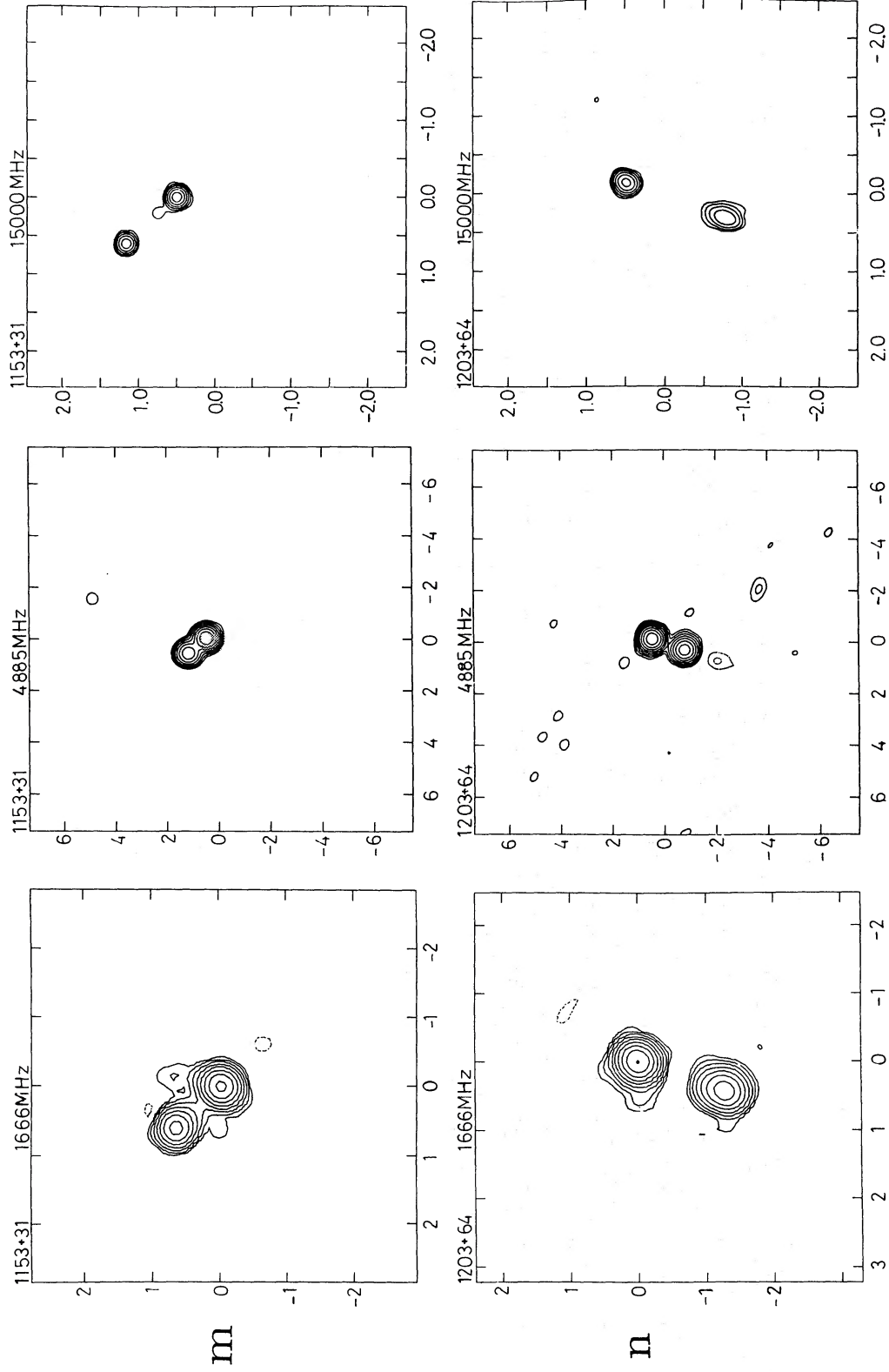


Figure 1 - continued

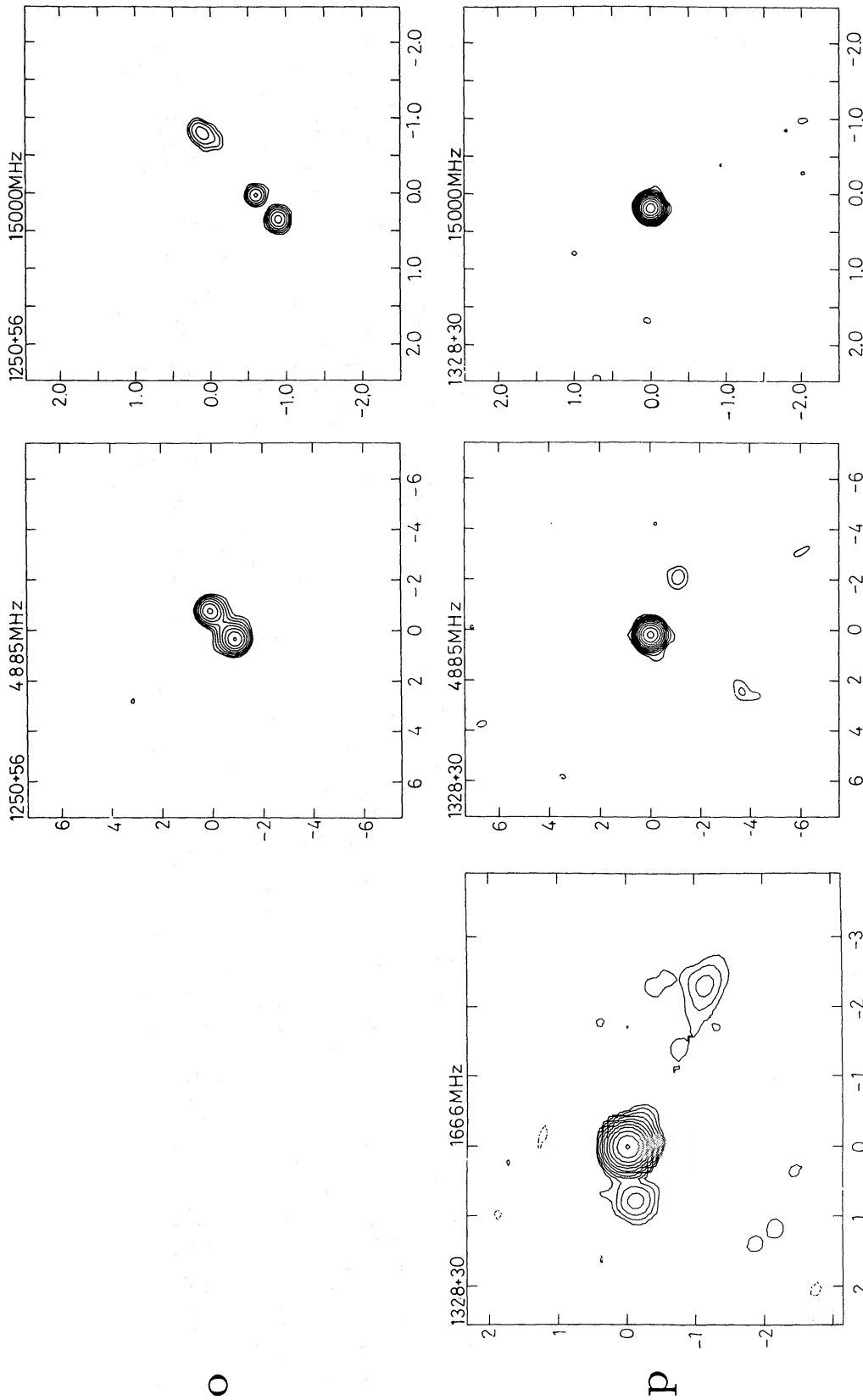


Figure 1 - continued

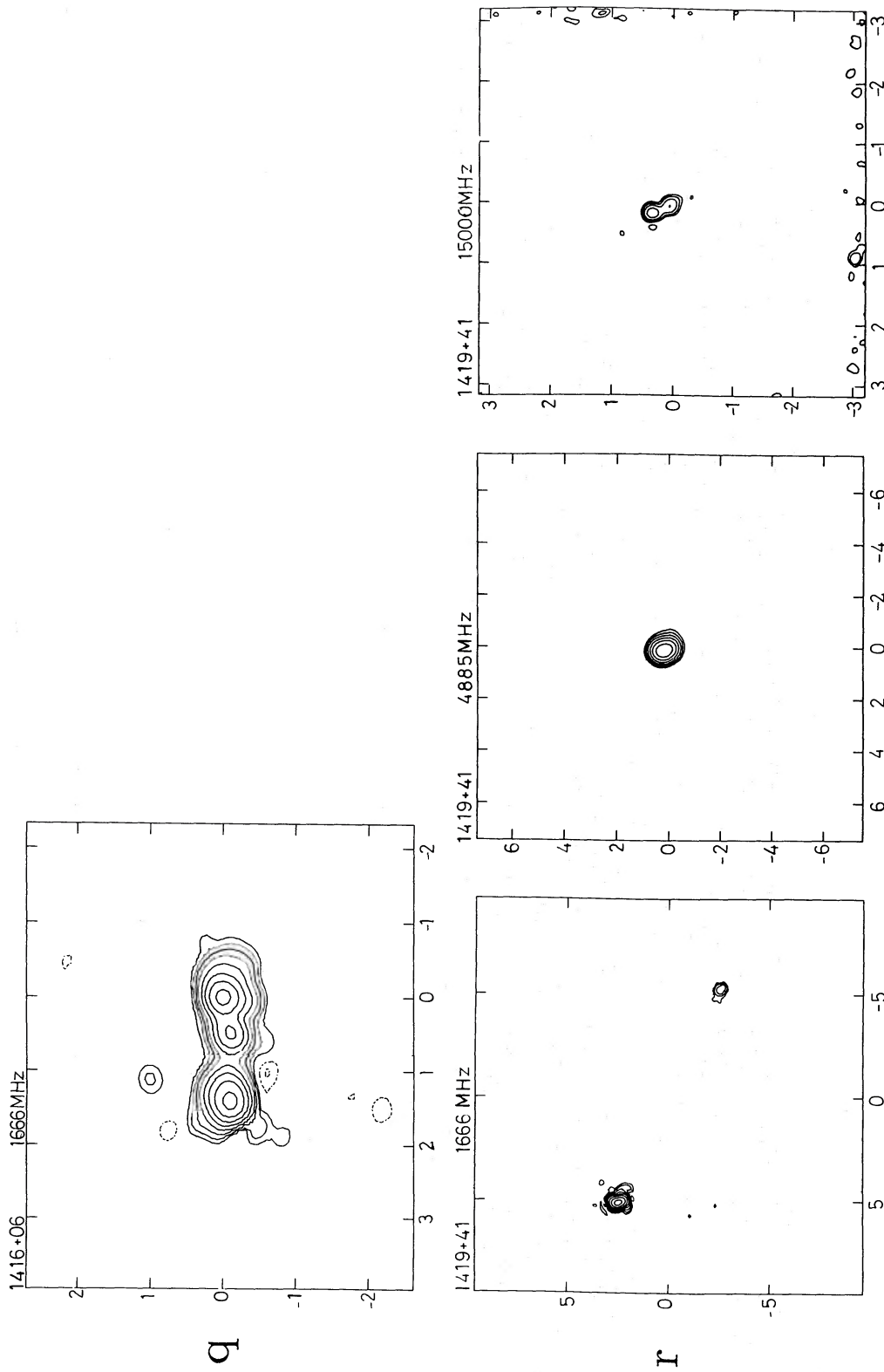


Figure 1 - continued

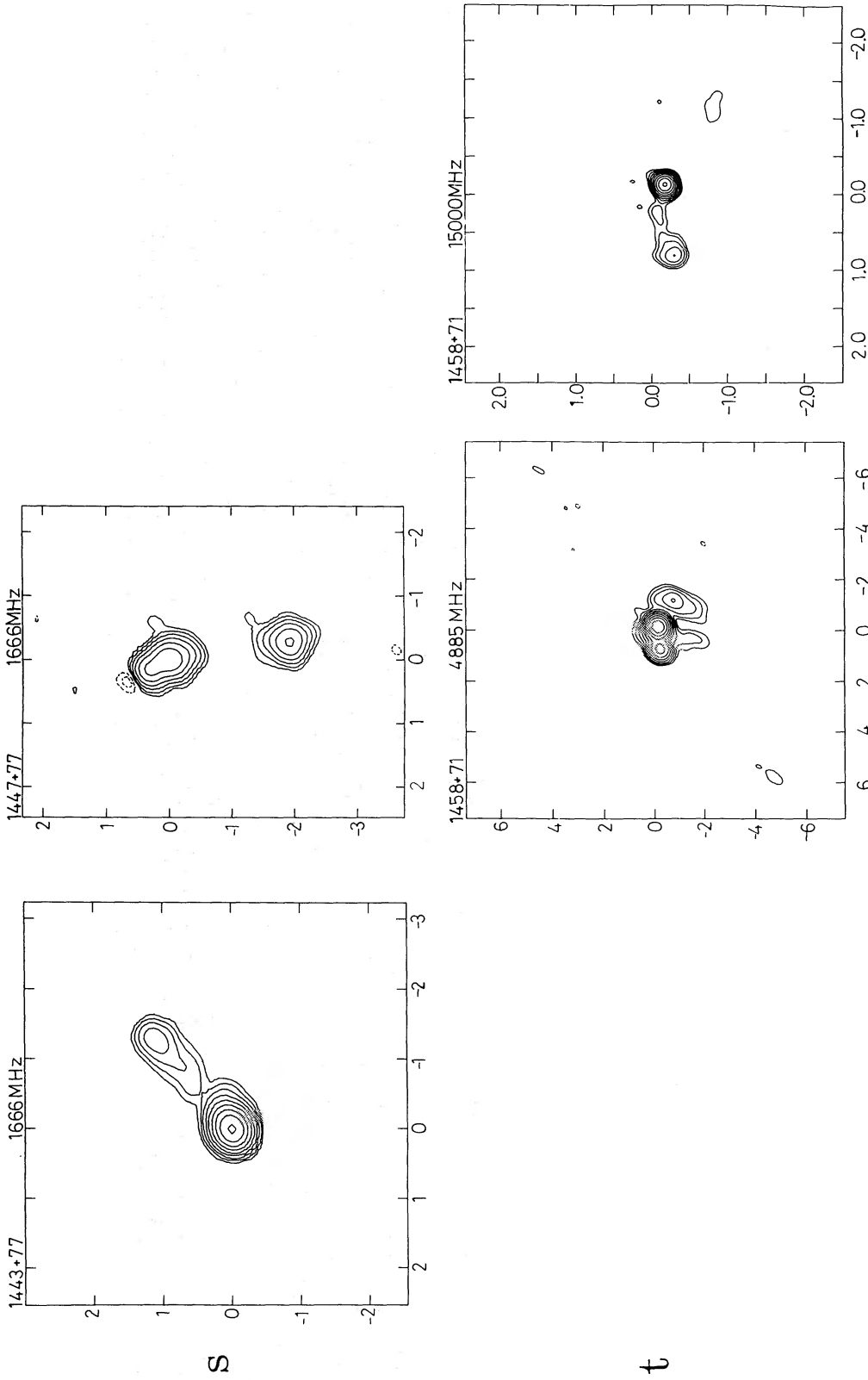


Figure 1 - continued

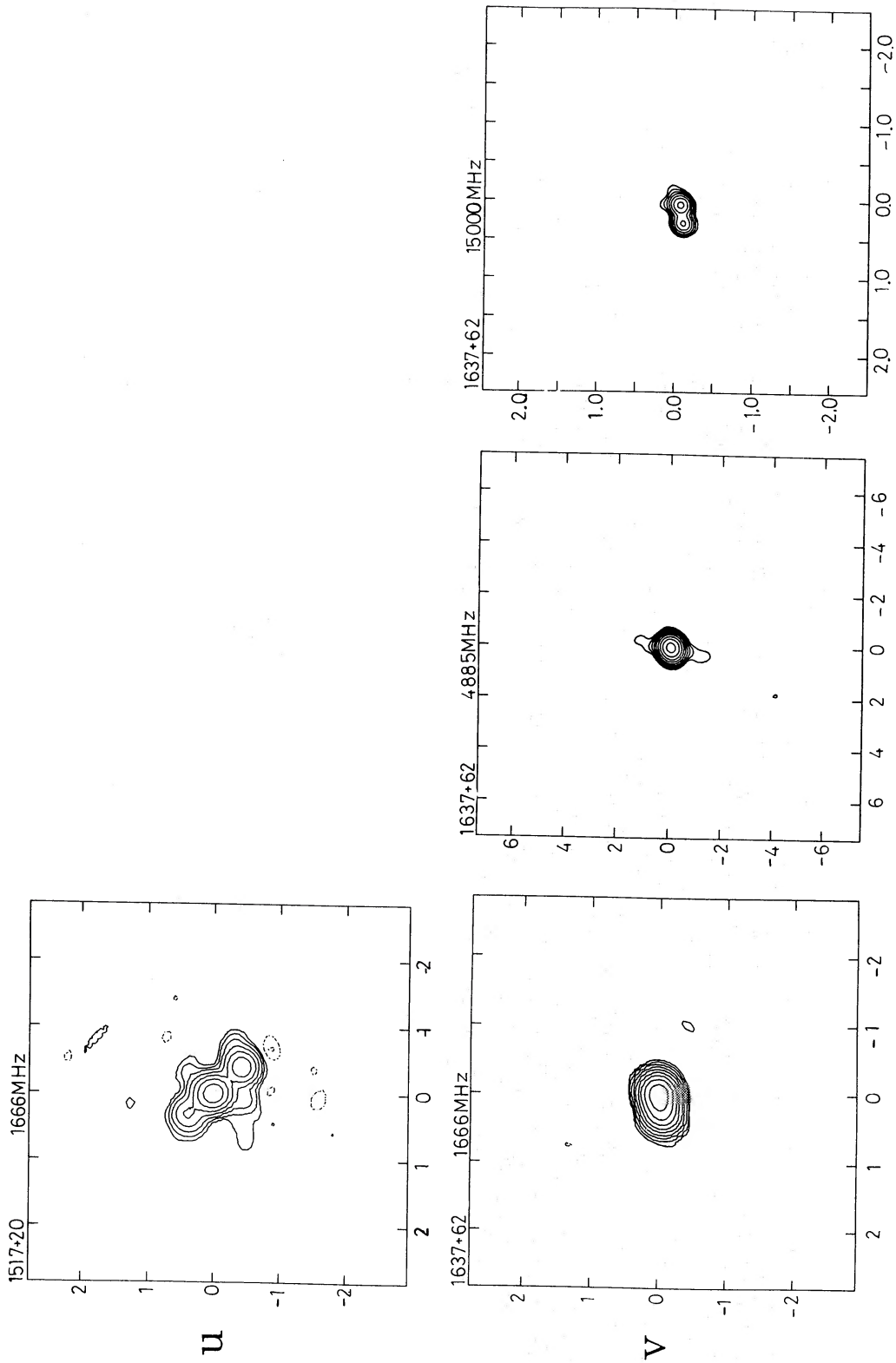


Figure 1 - continued

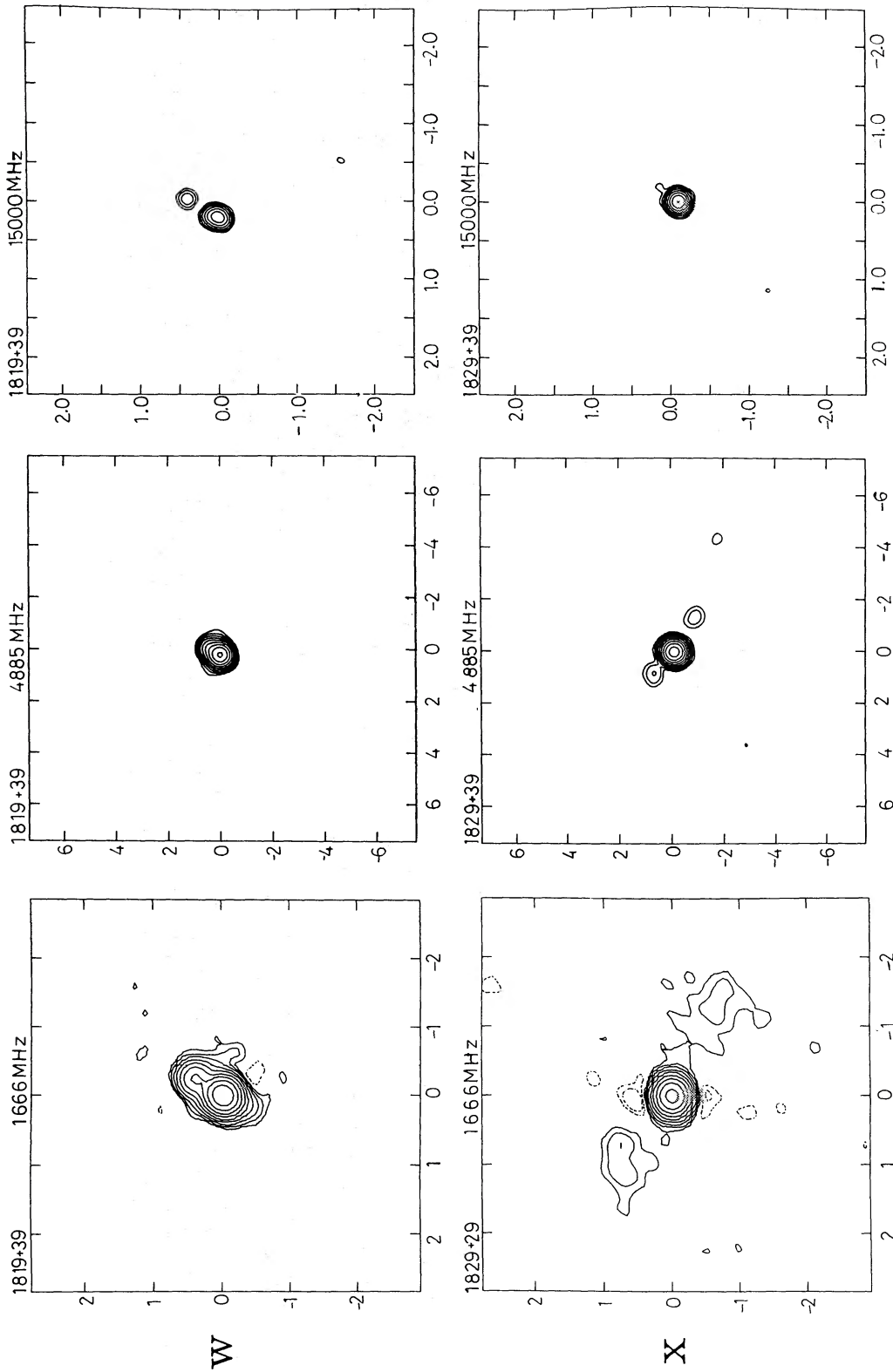


Figure 1 - continued

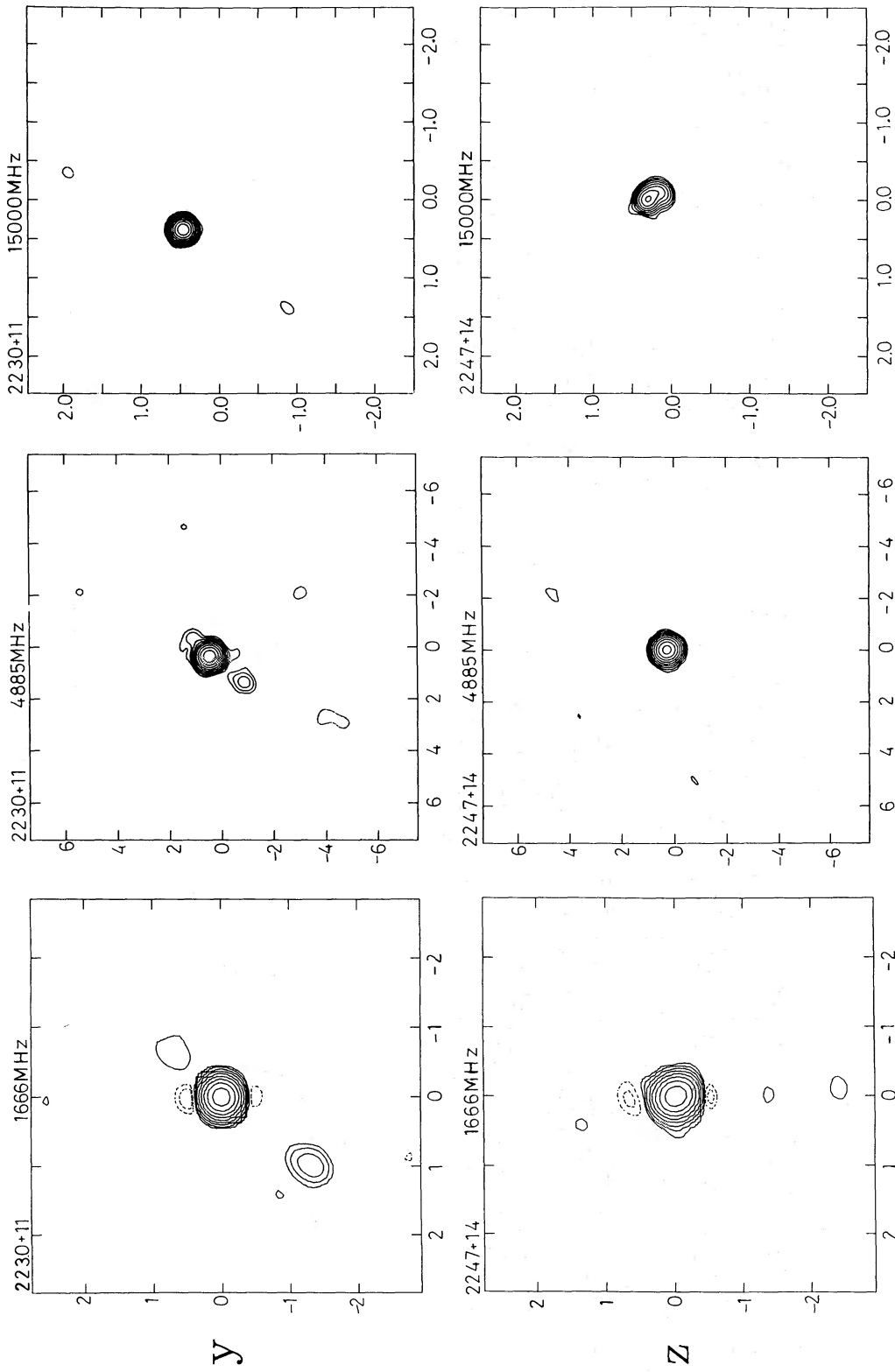


Figure 1 - continued

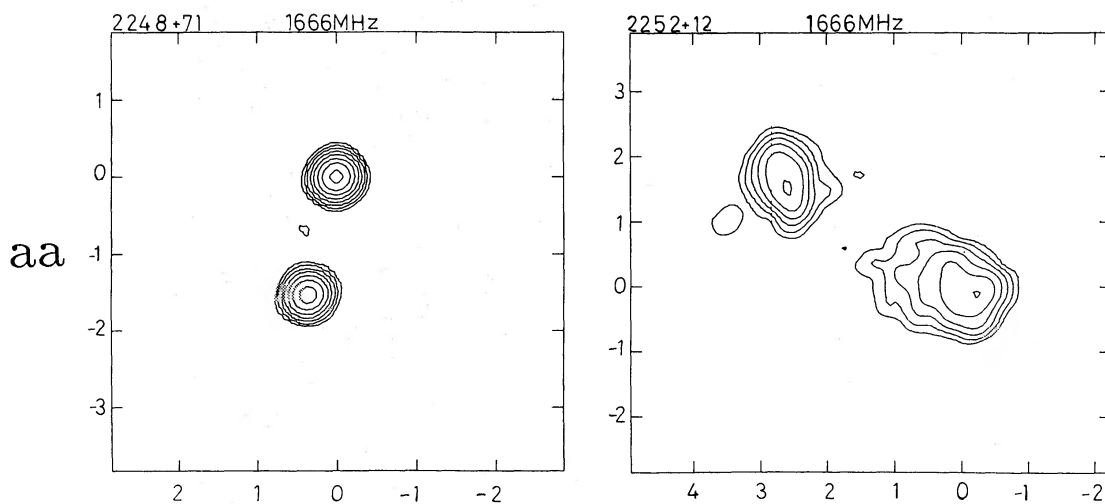


Figure 1 - continued

using the bottom contour. The resolution limit was taken to be one-third of the beam size, i.e. 0.1, 0.13 and 0.04 arcsec at 18, 6 and 2 cm, respectively. The letter 'u' means unresolved. Separations are given relative to the first component listed. Flux densities are either derived from the Gaussian fit or by integration over the component when it is well separated.

### 3.1 STRUCTURE

Column 5 of Table 1 gives a morphological classification based on the structure visible on the maps according to the following scheme:

P - point: largest angular size  $< 0.1$  arcsec at 18 or 2 cm, e.g. 0116 + 31. Note that two of these, CTA 21 and 4C 62.33, may be just resolved by the VLA at 2 cm.

S - single: resolved on longer baselines, but appearing as a single slightly extended component with angular size  $\geq 0.1$  arcsec, e.g. 3C 93.1.

D - double: a simple double source consisting of two components, sometimes with evidence for a low-level bridge of emission, e.g. 3C 67, 3C 237.

T - triple: sources where three components are aligned, e.g. 1829 + 29.

C - complex: sources with three or more components which are not aligned, e.g. 3C 43, 3C 286.

These classifications cannot be final since maps with higher resolution and/or improved dynamic range may result in the discovery of more components. Cases where a change of dynamic range or the availability of higher-resolution observations results in a change of morphological classification are noted in the following section. Such changes do not significantly alter our conclusions.

### 3.2 COMMENTS ON SOME INDIVIDUAL SOURCES

0127+23, 3C 43, *quasar*. The largest angular size in Table 1 is measured from the 18-cm map. A similar structure was obtained by Pearson *et al.* (1985). The northern component, at a separation of 2.5 arcsec from the bright core, has a steep spectrum and is not visible on the 2-cm map.

Table 2. Peak brightness and contour levels for the maps.

name	18 cm		6 cm		2 cm	
	Peak Jy/beam	min contour mJy/beam	Peak Jy/beam	min contour mJy/beam	Peak Jy/beam	min contour mJy/beam
0127+23	1.478	7.0	0.87	3.0	0.24	3.0
0134+32			4.34	7.0	0.94	7.0
0138+13	1.67	6.0	7.06	3.0	0.27	3.0
0221+27	1.22	10.0	0.52	3.0	0.10	3.0
0223+34	2.10	5.0	1.30	3.0	0.91	3.0
0316+16	7.01	14.0	2.91	5.0	0.85	5.0
0345+33	1.17	5.0				
0428+20	3.44	10.0	2.22	3.0	0.98	3.0
0518+16			3.10	5.0	0.51	5.0
0538+49			6.32	13.0	1.65	5.0
0658+38	8.72	5.0				
0858+29	0.24	4.0				
1005+07	2.77	6.0				
1019+22	0.73	4.0				
1143+50	2.04	7.0				
1153+31	1.52	10.0	0.61	5.0	0.15	3.0
1203+64	1.86	7.0	6.61	3.0	0.12	3.0
1250+56			0.40	3.0	0.13	3.0
1328+30	13.20	12.0	7.36	12.0	3.90	5.0
1416+06	1.36	8.0				
1419+41	1.08	6.0	0.17	3.0	0.06	5.0
1443+77	1.16	4.0				
1447+77	0.43	7.0				
1458+71			2.35	5.0	1.39	5.0
1517+20	1.12	10.0				
1637+62	2.76	6.0	1.04	3.0	0.23	3.0
1819+39	2.47	5.0	0.84	3.0	0.16	3.0
1829+29	2.39	7.0	1.11	3.0	0.39	3.0
2230+11	6.45	15.0	4.13	9.0	3.72	8.0
2247+14	1.55	7.0	1.01	3.0	0.44	3.0
2248+71	0.80	5.0				
2252+12	0.20	6.0				

Table 3. Unresolved sources (map not shown).

Name	Flux Density		
	18 cm	6 cm	2 cm
0116+31	2.62	1.55	0.91
0319+12	1.67	1.07	0.86
0404+76	5.39	2.89	1.60
0429+41	8.00		
1122+19	0.84		
1225+36	2.05	0.83	0.16
1323+32	4.60	2.42	1.21
1328+25	6.61	3.42	1.47
1345+12	4.93	3.11	1.78
1358+62	4.00	1.87	0.86
1413+34	1.84	1.03	0.48
1442+10	2.39	1.29	0.56
1600+33	2.92	2.13	1.50
1607+26	4.52	1.77	0.53
1634+62	4.14	1.55	0.45
2342+82	3.56	1.35	0.49

*0134+32, 3C 48, quasar.* A joint MERLIN/EVN observation of this source is being analysed (P. N. Wilkinson, private communication) and the MERLIN 18-cm data are not available to us. The 2-cm VLA map shows a complex structure and so we have labelled this source with a 'C' structure.

*0138+13, 3C 49, galaxy.* This source is best described as having 'double' structure, with the possibility of a low-brightness bridge connecting the two compact components. A third component, which may be a weak compact flat-spectrum core, is just visible on the 2-cm map. VLBI measurements (Fanti *et al.* 1985) show that the Eastern component may contain a compact hotspot at its outer edge. We have given the source a 'D' classification based on the MERLIN map.

*0221+27, 3C 67, galaxy.* The northern component of the double source contains complex structure visible at 2 cm. This has been fitted with two Gaussian components as listed in Table 4. VLBI measurements (Fanti *et al.* 1985) show that there is complex structure on the tens of mas scale in both components.

*0223+34, 4C 34.07, quasar?* We have doubts about the reality of the structure to the east of the brightest part of the source at 18 cm and have therefore given the source a 'D' classification. The object is identified as a possible quasar in PW1.

*0316+16, CTA 21, galaxy?* This source is slightly extended to the south-east on the 2-cm map, but model fitting of the visibility amplitudes shows that > 95 per cent of the flux density is

Table 4. Source parameters.

name	$S_{\text{ISEM}}$ Jy	sep "	pa °	$\omega_1$ "	$\omega_2$ "	pa °	$S_{6\text{cm}}$ Jy	sep "	pa °	$\omega_1$ "	$\omega_2$ "	pa °	$S_{2\text{cm}}$ Jy	sep "	pa °	$\omega_1$ "	$\omega_2$ "	pa °
0127+23	1.91			.2	.1	121	0.96			.2	.1	131	0.53			.3	.1	151
	0.15	2.50	-22	.4	.3	121	0.05	2.48	-22	.4	.3	107						
0134+32	0.51	0.87	63	.6	.3	59	0.13	0.85	67	.5	.3	67	0.03	0.85	64	.4	.2	154
							5.51			.3	.2	25	1.53		-154	.2	.1	23
0138+13	1.79			u			0.74			u			0.76	0.76	-154	.1	u	-154
	0.72	0.90	89	.3	.1	55	0.18	0.89	87	.3	.2	47	0.29			u		
0221+27	1.70			.2	.1	3	0.58			.2	.2	14	0.04	0.95	86	.2	.1	47
	0.98	2.10	-6	1.3	.6	174	0.25	2.20	-5	.5	.1	169	0.15			.1	.1	148
0223+34	2.10			u			0.10	1.80	-7	.7	.4	20	0.03	2.40	-5	.2	.1	145
	0.12	0.58	69	.3	.2	128	1.42			.2	.1	61	0.04	2.10	0	.2	.1	174
	0.34	0.50	-118	.1	.1	167	0.02	0.50	-118	u			1.0			.2	.1	118
0316+16	7.33			u			3.00			.1	u	174	0.01	0.50	-119	u		
0345+33	2.09			.3	.2	166	2.34			.1	u	160	0.86			u		
0428+20	3.77			.1	u	167	2.88			.4	.1	70	1.06			.1	u	165
0518+16							1.20	0.36	-109	.2	.1	65	0.76			.2	u	63
0538+49							7.49			.3	.2	41	0.38	0.35	-119	.1	u	68
0658+38	1.14			.2	.1	128							2.63	1.37	26	.2	.1	13
	0.32	2.46		.5	.4	52							0.18					
0858+29	0.30			.2	.2	-												
	0.35			1.2	.7	56												
1005+07	0.07	5.95	-18	.3	.2	147				.1	u	160				.1	u	165
	0.21	7.02	-11	1.6	.6	18				.4	.1	70	0.76			.2	u	63
	3.34			.2	.1	81				.2	.1	81	0.38			.1	u	68
1019+22	2.65	1.2	87	.2	.1	94				.2	.1	94	2.63			.2	u	55
	0.87			.2	u	83												
1143+50	0.65	0.81	81	.1	.1	-												
	0.55			.5	.1	19												
1153+31	0.57	4.16	177	.7	.3	176												
	1.78			.1	u	164	0.65			.1	.1	24	0.16			u		
	0.97	0.89	42	.1	u	43	0.31	0.90	41	.2	.1	24	0.08	0.90	43	u	u	43
													0.01	0.31	42	.2	u	17

Table 4 – continued

1203+64	2.17	1.33	162	.1	u	146	0.69	1.33	161	.1	u	54	0.17	1.34	161	.1	u	147
1250+56	1.06			.3	.2	161	0.34			.2	.2	116	0.11		161	.3	.1	164
							0.48			.3	.2		0.14			u	u	
1328+30	13.57			u			0.26	1.44	-49	.3	.2	132	0.05	0.44	-42	u	u	140
	0.20	0.76	101	.2	.2	-	7.66			.1	u		0.08	1.52	-49	.2	.1	
	0.27	2.55	-116	.6	.3	70	0.07	2.50	-116	.6	.5	92	4.07			u	u	
1416+06	1.93			.3	.2	99												
	0.74	0.50	100	.2	.1	106												
	2.20	1.39	93	.3	.2	97												
1419+41	2.59			.5	.2	15	0.26			.5	.3	19				.1	.1	41
	0.11	11.50	-116	.4	.2	48							0.11	0.31	-157	.2	.1	
1443+77	1.46			.2	.1	115							0.09					
	0.14	1.80	-41	1.1	.2	132												
1447+77	0.45			.3	.2	20												
	1.00	2.00	9	.6	.2	24												
1458+71							2.29			u	u		1.49			u	u	
	1.39	0.52	50	.2	.1	28	0.47	0.91	96	.2	u	140	0.15	0.93	97	.2	.1	78
	0.22	0.57	-136	.2	.1	67	0.20	1.20	-123	1.1	.3	160	0.04	1.19	-123	.4	.2	78
1517+20	0.70			.1	u	98	0.30	0.29	80	.6	.5	166	0.11	0.40	80	.9	.2	100
	2.72	0.25	100	.1	u	133												
1637+62	1.24			u	u		1.04			.2	.1	111				.1	u	126
	2.64	0.44	-27	u	u		0.20	.28	104	u	u		0.26		98	.1	u	123
1819+39	0.35			u	u		0.97			.3	.1	143	0.22			.1	u	159
	2.48	1.18	53	u	u		1.19			.1	.1		0.02	0.5	-32	u	u	91
1829+29	0.13	1.37	-115	.9	.4	98	0.02	1.15	47	.5	.2	93	0.43			.1	u	
	0.16	1.08	-43	1.2	.9	53	0.02	1.54	-120	.5	.3	52						
2230+11	6.46	0.95	-43	u	u		4.28			.1	u	114				u	u	
	0.08	1.63	143	.5	.3	137	0.06	0.91	-45	.6	.5	48						
2247+14	0.18			.3	.2	145	0.08	1.64	143	.4	.2	144						
2248+71	2.00			.2	.1	30	1.11			.2	.1	36				.2	.1	39
	0.83	1.57	167	u	u													
2252+12	0.50			.1	u	160												
	1.47	3.12	58	2.0	1.1	58												
	0.97			.8	.4	17												

from an unresolved component, and it is unresolved by MERLIN at 18 cm. For this reason we have labelled this object a 'P' source. VLBI observations by Jones (1984) indicate a 13-mas double in p.a.  $160^\circ$  at 6 cm, whereas Wilkinson *et al.* (1979) find a 20-mas double in the same position angle plus a fully resolved steep-spectrum component ( $> 30$  mas). Some evidence for this latter component may be present in our 6-cm model fitting; its angular size is about 100 mas and in a similar p.a. to that of the more compact structure. The complex structure indicates that this source is probably not a compact double as suggested by Jones.

*0429+41, 3C 119, quasar?* Recent VLBI measurements show this source to have very complex structure (Fanti *et al.* 1986; Nan *et al.* 1988), but it is essentially unresolved by MERLIN at 18 cm.

*0518+16, 3C 138, quasar.*

*0538+49, 3C 147, quasar.* These two objects have been well studied by VLBI (see for example Geldzahler *et al.* 1984; Simon, Readhead & Wilkinson 1984). Our maps of these two complex quasars are similar to those by van Breugel *et al.* (1984) and Pearson *et al.* (1985). Comprehensive maps of 3C 138 have been made by Fanti *et al.* (in preparation) using combined MERLIN and VLBI data at 6 cm.

*1328+30, 3C 286, quasar.* VLBI measurements of the core show the presence of a jet-like feature (Simon *et al.* 1980) 60 mas long pointing towards the component visible on our maps 2.6 arcsec away. The eastern component on our 18-cm map has a very steep spectrum and does not seem to be related to the VLBI structure. Its existence has been confirmed by P. Leahy (private communication) using an independent MERLIN data set.

*1419+41, 3C 299, galaxy.* The NE component only is shown on the maps at 6 and 2 cm.

*1607+26, CTD 93, galaxy.* This source is the archetype compact double (Mutel, Hodges & Phillips 1985). VLBI measurements show a double structure with a separation of 50 mas, so it is unresolved in our observations.

*1829+29, 4C 29.56 quasar?* This source has a dominant unresolved core with two lower brightness outer components symmetrically placed about the core, and is given a 'triple' classification. This structure is relatively common among the quasars of angular size in excess of a few arcseconds. Maps with very high dynamic range and improved resolution are needed to see if either or both of the lobes are fed by 'jets' as in many of the larger quasars.

*2230+11, CTA 102, quasar.* This object again has a triple structure. It has been extensively studied by VLBI and is one of the first low-frequency variable objects to be discovered. The VLBI structure found by Pearson, Readhead & Wilkinson (1980) consists of two components separated by 10 mas in position angle  $146^\circ$ . This position angle is close to that found for the direction of the south-east component 1.6 arcsec from the core and gives evidence for collimated energy supply to the outer lobes.

## 4 Discussion

The results presented here indicate the variety of structures shown by the compact steep-spectrum sources. These range from wide doubles, similar to the high-luminosity 'classical' double sources such as Cygnus A, to complex distorted structures. It is therefore unlikely that one simple model will suffice to explain this variety, and we may be dealing with several distinct types of object.

### 4.1 STRUCTURE VERSUS SELECTION FREQUENCY

One surprising feature of these observations is the discovery of a large number (17) of objects which are unresolved with MERLIN at 18 cm ( $< 0.1$  arcsec), in contrast to the results on the

3C CSS sources by Pearson *et al.* (1985), even though the resolution of the instruments used is similar. Most of these sources appear in the PW list and, in an attempt to eliminate any selection effects which may occur in the 3C sources listed in Table 1, we have generated a list of 3CR sources with the following criteria:

- (i) observed flux density at 178 MHz  $> 10$  Jy;
- (ii) high-frequency two-point (2.7–5 GHz) spectral index  $\geq 0.5$ ;
- (iii) angular size with  $\geq 80$  per cent of source flux density at 5 GHz of  $< 2$  arcsec;
- (iv)  $|b| > 10^\circ$ ,  $\delta > 10^\circ$ .

These criteria are the same as those of the Peacock & Wall sample, apart from the flux density limit and selection frequency.

Those sources in Table 1 listed as 'C' in column 3 comprise this 3CR subsample. The Peacock & Wall high-frequency sample can now be compared with a sample which is similar in angular size and luminosity of 2.7 GHz but selected at low frequency. Fig. 2 shows histograms of the numbers of various morphological types in the two samples. It is clear that the major differences are the larger proportion of point sources and smaller proportion of complex sources in the PW sample compared to the 3C list.

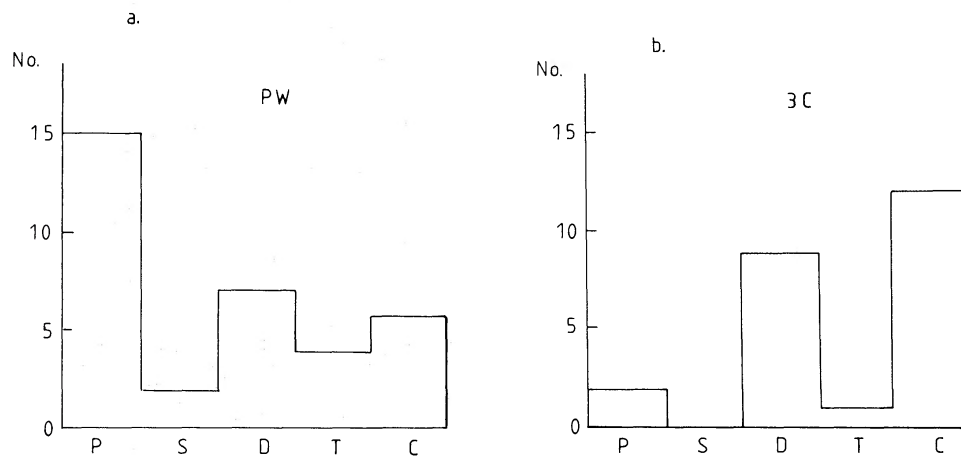


**Figure 2.** Histograms of morphological types for (a) the Peacock & Wall (PW2) sample and (b) the 3C sample of CSS. See Section 3.1 for the definition of morphological types.

The large number of compact sources found in centimetre-wavelength surveys is usually due to the presence of flat-spectrum objects ( $\alpha < 0.5$ ) which are known to be compact even on VLBI scales. It is possible that the PW CSS sources have spectra less steep than those of the 3CR CSS sources and therefore more compact sources appear in the sample by virtue of a rather arbitrary selection at  $\alpha = 0.5$ . Certainly, some of the PW CSS sources are 'normal' flat-spectrum sources erroneously included due to variability (particularly 0116+31 and 2230+11; van Breugel *et al.* 1984). Examination of the published spectra of the sources (e.g. Kellermann, Pauliny-Toth & Williams 1969; Kuhr *et al.* 1981) shows that the point sources in the PW sample have a median high-frequency (2.7–5 GHz) spectral index of  $0.65 \pm 0.04$ , while the median spectral index for the extended sources is  $0.77 \pm 0.05$ . This can be compared with the value of  $0.67 \pm 0.03$  for the PW CSS sources as a whole and  $0.83 \pm 0.05$  for the 3C CSS sources, which are mostly extended. Thus the PW point sources are not significantly less steep

than the PWCSS sample as a whole, implying that contamination by compact flat-spectrum sources is small. The 3C CSS sources are significantly steeper. This is consistent with the larger number of complex sources found in the 3C sample if extended steep-spectrum emission is present, as is the case in sources such as 3C 147 (Simon *et al.* 1980), but it does not explain the excess of point sources in the PW sample.

The low-frequency spectra, however, are on the whole quite different for the point sources. Estimates from published flux density data (Kuhr *et al.* 1981; Roger, Costain & Stewart 1986; Readhead & Hewish 1974) of the frequencies at which the spectra become flat ( $\alpha \sim 0$ ) are given in Table 1. The majority of the point sources show a clear low-frequency turnover, with the peak flux density occurring predominantly at a frequency between 300 and 1000 MHz (see Fig. 3). These sources are therefore missing from the 3CR sample due to their low flux densities at 178 MHz, but they occur in the PW sample and give rise to the larger proportion of compact steep-spectrum sources found in the high-frequency surveys, as discussed by Peacock & Wall 1982. The addition of these point sources to the 3CR sample would result in the relative proportion of CSS sources in the PW and 3CR sample becoming similar, so there is no need to resort to luminosity versus size or luminosity versus  $\alpha$  effects in order to explain the difference in fractions of CSS sources contained in high- and low-frequency surveys.

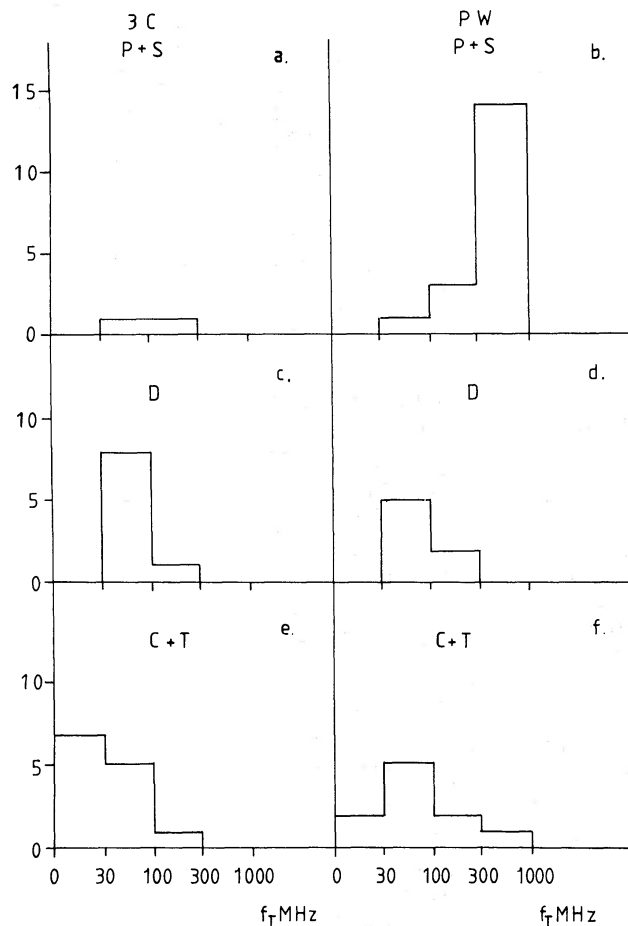


**Figure 3.** Histograms of turnover frequency for the 3C and PW2 samples of CSS. (a) and (b) are for the unresolved and slightly resolved sources (P and S), (c) and (d) for the double sources (D), and (e) and (f) for the complex and triple sources (C and T).

## 4.2 LUMINOSITY EFFECTS

A comparison of the redshift distributions of the various structural types shows no significant difference between the 3C and Peacock & Wall samples, so the point sources are physically smaller, at least in projected linear size. Similarly the monochromatic luminosities at 2.7 GHz are not significantly different, whereas the complex sources are more luminous as shown in Table 5. (Since there are only two P and S sources in the 3C sample, the average luminosity is not very meaningful.) We cannot therefore ascribe the lack of point sources in the 3C sample to a distance or luminosity effect at a fixed angular resolution. The main difference between the two samples is thus caused by spectral turnover and not by luminosity effects. Henceforth we merge the samples to study further properties of the sources.

Table 5. Mean logarithmic luminosities.

Morphology	3C	PW
	log (P)	log (P)
P & S	26.56±1.0	25.96±0.23
D	25.76±0.21	25.64±0.19
C	26.28±0.16	26.50±0.10

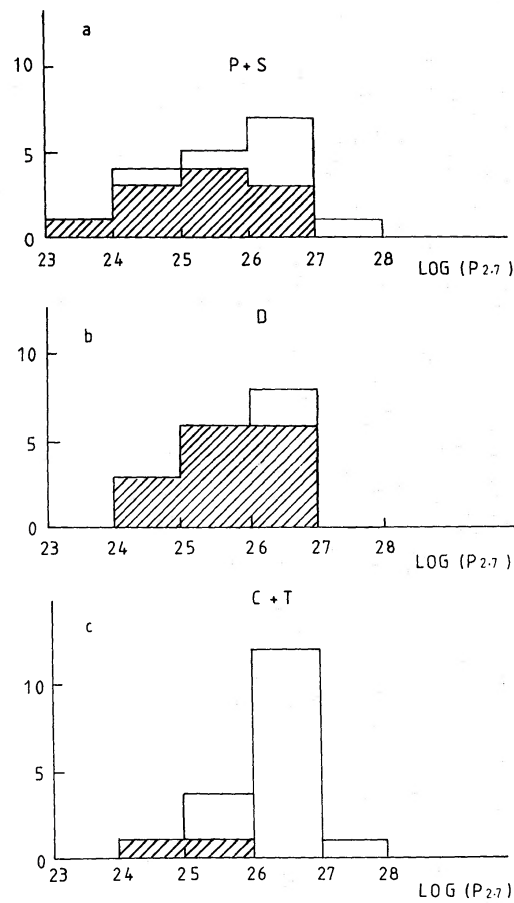
## 4.3 OPTICAL IDENTIFICATION AND RADIO STRUCTURE

Fig. 4 shows histograms of luminosity for sources of different morphological type. Identifications have been taken from Spinrad *et al.* (1985) and Peacock & Wall (1981), supplemented by the identification of 0316+16 (Allen, Wright & Ables 1982) and redshifts for 0319+12, 0428+20 and 2248+71, 1323+32 and 1358+62, and 2342+82 (private communications from H. Kuhr, H. Spinrad, J. Dunlap and C. Lawrence, respectively). A P or S source is equally likely to be a galaxy, quasar or unidentified. The double sources are predominantly galaxies whereas the sources with complex structures are almost entirely quasars. The higher luminosity for the C sources can be seen clearly, as expected for quasars.

The more complex structure of quasars was noticed for a smaller sample of sources by Wilkinson *et al.* (1984b), and it is important to find out if this effect, present in both the 3C and PW samples, is due to projection or is an intrinsic property of galaxies and quasars. Note that the effect still occurs in the luminosity range of  $10^{26}$ – $10^{27}$  W Hz<sup>-1</sup> sr<sup>-1</sup> where the galaxies and quasars overlap. This indicates that the effect is correlated with optical type rather than just luminosity alone.

## 4.4 WHY DO QUASARS HAVE COMPLEX STRUCTURES?

A possible explanation for the morphological differences between radio galaxies and quasars is that powerful radio galaxies are quasars seen in projection. The basic idea (Barthel 1989) is that quasars, when seen with their radio axes in the plane of the sky, have their strong nuclear continuum emission and broad emission lines hidden from view. Only when the angle to the line-of-sight becomes about 45° does the object become recognizable as a quasar. This accounts fairly naturally for several of the statistical properties of radio galaxies and quasars, e.g. radio galaxies are on average larger in linear size than quasars, and cores and jets are more dominant in quasars (Doppler boosting). In the present context it can account for the greater complexity amongst quasar structures, since small angles to the line-of-sight magnify bends in



**Figure 4.** Histograms of the logarithm of the monochromatic luminosity of 2.7 GHz in  $\text{W Hz}^{-1} \text{sr}^{-1}$  for (a) P and S, (b) D, and (c) C and T sources. Galaxies are shown shaded.

the structure, and the greater prominence of cores and jets due to Doppler boosting will complicate the overall structure.

Not only do compact sources fit this picture, but recent studies of the low-brightness bridges in quasars and radio galaxies of large angular size show similar effects (Leahy, Muxlow & Stephens 1989). They find that the bridges between the lobes in quasars are more distorted and fatter than in radio galaxies. Of course, not everything fits so well (see discussion in Scheuer 1987).

An alternative explanation is that, as in the case of the galaxies, these quasars are physically small and the distortion is intrinsic and not due entirely to projection effects. Such distortion could be caused by rapid precession or rotation in the quasars over time-scales of less than the largest linear size/ $c$ , i.e.  $< 10^5$  yr. This is shorter than normal galaxy rotation periods, but comparable with precessional time-scales of galactic nuclei (Gower *et al.* 1982).

Interaction of the jets and radio components with the interstellar medium can also cause distorted structures. Typical minimum pressures in the radio components in the quasars vary from  $10^{-9}$  to  $10^{-8} \text{N m}^{-2}$ . The densities and temperatures of gas typically found in the narrow-line region of quasars (Heckman *et al.* 1984) will give sufficient pressure to deflect these jets. van Breugel *et al.* (1984) point out that the CSS sources have lower polarization at 6 cm than sources in general, suggesting the presence of relatively dense ionized gas causing Faraday depolarization. This gas can also give rise to a low-frequency turnover at about 100 MHz via free-free absorption with emission measures of  $\sim 10^6 \text{cm}^{-6} \text{pc}$ . We would there-

fore expect the doubles which seem to have low distortion to have higher polarization and lower turnover frequencies than the complex sources, if in regions of lower gas density. However, examination of the polarization data of Tabara & Inoue (1980) shows that six of the 12 double galaxies have a polarization at 6 cm of  $\leq 2$  per cent, compared to six of the 13 complex quasars. Note also that Saikia, Singal & Cornwell (1987) find that the CSS cores of quasars are significantly more polarized at 6 cm than those of galaxies. Fig. 3 shows that the double sources (mainly galaxies) have, if anything, slightly higher turnover frequencies than the complex sources (quasars). The double sources therefore do not appear to contain less gas and we cannot conclude that distorted structures necessarily result from interactions with interstellar gas, unless this gas is dynamically active in quasars and not in galaxies.

#### 4.5 THE RADIO SPECTRUM

Synchrotron self-absorption can also give rise to low-frequency turnover in the radio spectra. Indeed, this is almost certainly occurring in the 'point' sources, where the observed brightness temperatures are  $> 10^8$  K at 18 cm and the angular sizes, calculated from the low-frequency turnover frequencies and assuming equipartition between magnetic and particle energies (Scott & Readhead 1977), are consistent with the upper limits ( $< 0.1$  arcsec) found in our observations.

The brightness temperatures of the components of the extended sources are typically  $\sim 10^7$  K at 18 cm and their angular sizes are generally consistent with equipartition. The slightly lower turnover in the complex sources compared with the doubles may be due to the presence of more extended emission (as in the case of 3C 380, Wilkinson *et al.* 1984a) in the sources with complex structures. An extensive spectral decomposition is needed to obtain detailed information on the physical conditions in each component of these sources, which is beyond the scope of this paper, but the typical parameters of the components listed in Table 4 indicate that the equipartition magnetic fields are  $\sim 30$  nT and minimum pressures  $\sim 10^{-9}$  N m $^{-2}$ . Furthermore, the observed turnover frequencies are consistent with equipartition between magnetic and particle energies. This again indicates that free-free absorption does not play a major role in the formation of the source spectra.

For all sources listed in Table 4 for which two or three frequency measurements are available, we computed the components' spectral indices between 18 and 6 cm and between 6 and 2 cm. No flat-spectrum components are revealed by this analysis. Therefore any compact core, if present, must still be embedded in a stronger extended component, and is undetected in our observations. In double sources, the two components have similar spectral indices. The spectra, on average, steepen by  $\sim 0.2$  in the high-frequency interval. This steepening could be due to flux scale uncertainties and/or to resolution effects, mostly at 2 cm. But it could also be genuine and represent the continuation of the bending observed at low frequencies.

## 5 Conclusion

Our studies of the radio structures of compact steep-spectrum sources from the 3C and Peacock & Wall (1981) surveys show that the lack of unresolved ( $< 0.1$  arcsec) objects in the former survey is due to the presence of low-frequency absorption in many of these objects. Sources with double structures are predominantly identified with galaxies (80 per cent), whereas the sources with complex structure are almost entirely quasars (93 per cent). We find that this basic difference in structure cannot be explained simply in terms of interaction with a dense interstellar gas in quasars. Projection effects, with the jets in quasars being more in the line-of-sight than those in galaxies, could explain the observed structures, but other features

related to relativistic beaming should be present that are not observed. Further studies, particularly using VLBI techniques on the unresolved objects in these samples, may help resolve this problem. Indeed, it is intriguing to note that 3C 119, a probable quasar, has a highly distorted structure (Fanti *et al.* 1986) on the scale of 0.1 arcsec whereas CTD 93, a galaxy, has a double structure with a separation of 0.05 arcsec (Phillips & Shaffer 1983).

### Acknowledgments

The authors thank the many people who have assisted in the preparation of the maps and for discussions of the results. R. E. Spencer thanks the Istituto di Radioastronomia and the Dipartimento di Astronomia, Bologna for hospitality during the preparation of this paper.

### References

- Allen, D. A., Wright, A. E. & Ables, J. G., 1982. *J. Astrophys. Astr.*, **3**, 189.
- Baars, J. W. M., Genzel, R., Pauliny-Toth, I. I. K. & Witzel, A., 1977. *Astr. Astrophys.*, **61**, 99.
- Barthel, P. D., 1989. *Astrophys. J.*, **336**, 606.
- Cawthorne, T. V., Scheuer, P. A. G., Morison, I. & Muxlow, T. W. B., 1986. *Mon. Not. R. astr. Soc.*, **219**, 883.
- Cornwell, T. J. & Wilkinson, P. N., 1981. *Mon. Not. R. astr. Soc.*, **196**, 1067.
- Cornwell, T. J. & Wilkinson, P. N., 1983. In: *Indirect Imaging*, p. 207, ed. Roberts, J. A., Cambridge University Press.
- Davis, R. J., Muxlow, T. W. B. & Conway, R. G., 1985. *Nature*, **318**, 343.
- Davis, R. J., Stannard, D. & Conway, R. G., 1977. *Nature*, **267**, 596.
- Fanti, C., Fanti, R., Parma, P., Nan, R., Schilizzi, R. T., Spencer, R. E., van Breugel, W. J. M. & Venturi, T., 1988. In: *Impact of VLBI on Astrophysics and Geophysics, IAU Symp. No. 129*, p. 111, eds Reid, M. J. & Moran, J. M., Kluwer, Dordrecht.
- Fanti, C., Fanti, R., Parma, P., Schilizzi, R. T. & van Breugel, W. J. M., 1985. *Astr. Astrophys.*, **143**, 292.
- Fanti, C., Fanti, R., Schilizzi, R. T., Spencer, R. E. & van Breugel, W. J. M., 1986. *Astr. Astrophys.*, **170**, 10.
- Geldzahler, B., Fanti, C., Fanti, R., Schilizzi, R. T., Shaffer, D. & Weiler, K. W., 1984. *Astr. Astrophys.*, **131**, 232.
- Gower, A. C., Gregory, P. C., Hutchings, J. B. & Ursula, W. G., 1982. *Astrophys. J.*, **262**, 478.
- Hargrave, P. J. & Ryle, M., 1974. *Mon. Not. R. astr. Soc.*, **166**, 305.
- Heckman, T. M., Miley, G. K. & Green, R. F., 1984. *Astrophys. J.*, **281**, 525.
- Högbom, J. A., 1974. *Astr. Astrophys. Suppl.*, **15**, 417.
- Jenkins, C. J., Pooley, G. G. & Riley, J. M., 1977. *Mem. R. astr. Soc.*, **84**, 61.
- Jones, D. L., 1984. *Astrophys. J.*, **276**, L5.
- Kapahi, V. K., 1981. *Astr. Astrophys. Suppl.*, **43**, 381.
- Kellermann, K. I., Pauliny-Toth, I. I. K. & Williams, P. J. S., 1969. *Astrophys. J.*, **157**, 1.
- Kuhr, H., Witzel, A., Pauliny-Toth, I. I. K. & Nauber, U., 1981. *Astr. Astrophys. Suppl.*, **45**, 367.
- Leahy, P. D., Muxlow, T. W. B. & Stephens, P. W., 1989. *Mon. Not. R. astr. Soc.*, **239**, 401.
- Mutel, R. L., Hodges, M. W. & Phillips, R. B., 1985. *Astrophys. J.*, **240**, 88.
- Nan Ren-dong, Schilizzi, R. T., Fanti, C., Fanti, R., van Breugel, W. J. M. & Muxlow, T. W. B., 1988. In: *The Impact of VLBI on Astrophysics and Geophysics, IAU Symp. No. 129*, p. 119, eds Reid, M. J. & Moran, J. M., Kluwer, Dordrecht.
- Peacock, J. A. & Wall, J. V., 1981. *Mon. Not. R. astr. Soc.*, **194**, 331.
- Peacock, J. A. & Wall, J. V., 1982. *Mon. Not. R. astr. Soc.*, **198**, 843.
- Pearson, T. J., Perley, R. A. & Readhead, A. C. S., 1985. *Astr. J.*, **90**, 738.
- Pearson, T. J., Readhead, A. C. S. & Wilkinson, P. N., 1980. *Astrophys. J.*, **236**, 714.
- Pedlar, A., Unger, S. W., Axon, D. J. & Dyson, J. E., 1987. In: *Star Formation in Galaxies*, ed. Persson, C. J. L., NASA Conf. Publ. 2466.
- Perley, R. A., Dreher, J. W. & Cowan, J. J., 1984. *Astrophys. J.*, **285**, L35.
- Phillips, R. B. & Shaffer, D. B., 1983. *Astrophys. J.*, **271**, 32.
- Readhead, A. C. S. & Hewish, A., 1974. *Mem. R. astr. Soc.*, **78**, 1.
- Readhead, A. C. S. & Wilkinson, P. N., 1978. *Astrophys. J.*, **223**, 25.
- Roger, R. S., Costain, C. H. & Stewart, O. J., 1986. *Astr. Astrophys. Suppl.*, **65**, 485.
- Saikia, D. J., Singal, A. K. & Cornwell, T. J., 1987. *Mon. Not. R. astr. Soc.*, **224**, 379.
- Scheuer, P. A. G., 1987. In: *Superluminal Radio Sources*, p. 104, eds Zensus, J. A. & Pearson, T. J., Cambridge University Press.

- Scott, M. A. & Readhead, A. C. S., 1977. *Mon. Not. R. astr. Soc.*, **180**, 539.
- Simon, R. S., Readhead, A. C. S., Moffet, A. T., Wilkinson, P. N. & Anderson, B., 1980. *Astrophys. J.*, **236**, 707.
- Simon, R. S., Readhead, A. C. S. & Wilkinson, P. N., 1984. In: *VLBI and Compact Radio Sources, IAU Symp. No. 110*, p. 111, eds Fanti, R., Kellermann, K. & Setti, G., Reidel, Dordrecht.
- Spinrad, H., Djorgovski, S., Marr, J. & Aguilar, L., 1985. *Publs astr. Soc. Pacif.*, **97**, 932.
- Tabara, H. & Inoue, M., 1980. *Astr. Astrophys. Suppl.*, **39**, 379.
- van Breugel, W., Miley, D. K. & Heckman, T., 1984. *Astr. J.*, **89**, 5.
- Wilkinson, P. N., Booth, R. S., Cornwell, T. J. & Clark, R. R., 1984a. *Nature*, **308**, 619.
- Wilkinson, P. N., Readhead, A. C. S., Anderson, B. & Purcell, G. H., 1979. *Astrophys. J.*, **232**, 365.
- Wilkinson, P. N., Spencer, R. E., Readhead, A. C. S., Pearson, T. J. & Simon, R. S., 1984b. In: *VLBI and Compact Radio Sources, IAU Symp. No. 110*, p. 25, eds Fanti, R., Kellermann, K. & Setti, G., Reidel, Dordrecht.